



HAL
open science

1H, 13C, 15 N backbone and side-chain NMR assignments for three MAX effectors from *Magnaporthe oryzae*

Mounia Lahfa, André Padilla, Karine de Guillen, Joana Pissarra, Mouna Raji, Stella Cesari, Thomas Kroj, Pierre Gladieux, Christian Roumestand, Philippe Barthe

► To cite this version:

Mounia Lahfa, André Padilla, Karine de Guillen, Joana Pissarra, Mouna Raji, et al.. 1H, 13C, 15 N backbone and side-chain NMR assignments for three MAX effectors from *Magnaporthe oryzae*. *Biomolecular NMR Assignments*, 2022, 16 (2), pp.305-309. 10.1007/s12104-022-10095-2. hal-04234517

HAL Id: hal-04234517

<https://hal.science/hal-04234517>

Submitted on 13 Oct 2023

HAL is a multi-disciplinary open access archive for the deposit and dissemination of scientific research documents, whether they are published or not. The documents may come from teaching and research institutions in France or abroad, or from public or private research centers.

L'archive ouverte pluridisciplinaire **HAL**, est destinée au dépôt et à la diffusion de documents scientifiques de niveau recherche, publiés ou non, émanant des établissements d'enseignement et de recherche français ou étrangers, des laboratoires publics ou privés.

¹H, ¹³C, ¹⁵N Backbone and side-chain NMR assignments for three MAX effectors from *Magnaporthe oryzae*.

Mounia Lahfa¹, André Padilla¹, Karine de Guillen¹, Joana Pissarra¹, Mouna Raji¹, Stella Cesari², Thomas Kroj², Pierre Gladieux², Christian Roumestand^{1*}, and Philippe Barthe¹.

¹Centre de Biologie Structurale, Univ Montpellier, INSERM U1054, CNRS UMR 5048, Montpellier France.

²PHIM Plant Health Institute, Univ Montpellier, INRAE, CIRAD, Institut Agro, IRD, Montpellier, France.

* Correspondence: christian.roumestand@cbs.cnrs.fr

Abstract

Effectors are small and very diverse proteins secreted by fungi and translocated in plant cells during infection. Among them, MAX effectors (for *Magnaporthe* AvrS and ToxB) were identified as a family of effectors that share an identical fold topology despite having highly divergent sequences. They are mostly secreted by ascomycetes from the *Magnaporthe* genus, a fungus that causes the rice blast, a plant disease leading to huge crop losses. As rice is the first source of calories in many countries, especially in Asia and Africa, this constitutes a threat for world food security. Hence, a better understanding of these effectors, including structural and functional characterization, constitutes a strategic milestone in the fight against phytopathogen fungi and may give clues for the development of resistant varieties of rice. We report here the near complete ¹H, ¹⁵N and ¹³C NMR resonance assignment of three new putative MAX effectors (MAX47, MAX60 and MAX67). Secondary structure determination using TALOS-N and CSI.3 demonstrates a high content of β-strands in all the three proteins, in agreement with the canonic β-sandwich structure of MAX effectors. This preliminary study provides foundations for further structural characterization, that will help in turn to improve sequence predictions of other MAX effectors through data mining.

Keywords

Magnaporthe oryzae, effector, plant pathogen, Protein chemical shift assignment

Biological Context

Phytopathogenic fungi cause ravaging diseases that constitute a threat to agriculture and food security. Among the large variety of pathogens, the ascomycete *Magnaporthe oryzae* causes the rice blast, the most destructive disease of rice worldwide (Ou 1980). This pathogen is a hemi biotrophic organism, starting its infection by growth and colonization of the plant and then entering a necrotic phase (Dean et al. 2012; Fernandez and Orth 2018) responsible for the crop's damages and losses (Hogenhout et al. 2009; Jones and Dangl 2006; Doehlemann et al. 2014). Beside rice, several other cereal cultures are impacted, including wheat, barley and millet (Couch et al. 2005).

Even if resistance appears in some cultures, the fungus generally escapes this blast resistance (Araújo et al. 2000) by secreting during infection an extended repertoire of small proteins (size under 200 amino acids) named effectors, whose specific targets remain only partially known. Effectors show very divergent sequences, sharing a signal peptide on the N-terminal end. This signal peptide is essential for their secretion and then their translocation inside the plant cell (Petre and Kamoun 2014). These translocation mechanisms remain mostly unknown but it has been shown that effector secretion can be dependent on the conventional secretory pathway of the plant, or dependent on another secretion system from the pathogen itself (Ribot et al. 2012; Giraldo et al. 2013; Eseola et al. 2021). They constitute a way to escape basal resistance based on PAMP/MAMP recognition by extra-cellular cell surface receptors (Wang et al. 2014). Some effectors can also prevent recognition of effectors by specific resistance proteins, hindering the protecting immune response (Houterman et al. 2008).

In 2015, a new family of effectors, called MAX-effectors (for *Magnaporthe* *Avrs* and *ToxB* like) was identified from bioinformatic analysis (de Guillen et al. 2015) and the 3D structure has been solved for several of them (Zhang et al. 2013; Nyarko et al. 2014; Maqbool et al. 2015; de Guillen et al. 2015, De la Concepcion et al. 2018, 2021; Zhang et al. 2018; Maidment et al. 2021; Bentham et al. 2021). Despite having low sequence identity (generally under 25 %), they share a conserved structure and topology consisting of a sandwich made of five to six antiparallel β strands (Zhang et al. 2013; Nyarko et al. 2014). These MAX-effectors also show two highly conserved cysteines forming a disulphide bond between the two sheets (de Guillen et al., 2015). Restricting the analysis to the genomes of *Magnaporthe* genus, where most of MAX effectors were identified, a new prediction pipeline (to be published elsewhere) allows us to extract new MAX candidates, among them MAX47, MAX60 and MAX67. We report here the backbone and side-chain resonance assignments of these three effectors. These assignments will provide the foundation for their 3D structure determination, and will allow interaction studies with their putative targets.

Methods and Experiments

Recombinant protein expression and purification.

Uniformly labeled (^{15}N and $^{15}\text{N}/^{13}\text{C}$) proteins (MAX47, MAX60 and MAX67) were expressed in *E. coli* BL21 (DE3) cells (Invitrogen, Thermo Fisher Scientific, Waltham, USA) from a homemade plasmid pDB-his-CCDB-3C (courtesy of Frederic Allemand, CBS Montpellier, France) allowing expression of the recombinant fusion proteins with a His₆-tag cleavable by the protease HRV 3C. In the three constructs, the N-terminal signal peptide has been removed from the original sequence, yielding final proteins of 95, 89 and 60 residues long for MAX47, MAX60 and MAX67, respectively.

Protein expression was carried out in $^{15}\text{NH}_4\text{Cl}$ (1 g/l) or $^{15}\text{NH}_4\text{Cl}$ (1 g/l) / ^{13}C -Glucose (3 g/l) enriched M9 medium. Cells were grown at 37°C until reaching an $\text{OD}_{600} = 0.8$ and then, expression proceeded overnight at 30°C after induction by addition of 0.3 mM IPTG. Cells were harvested by centrifugation, resuspended in denaturing buffer (50 mM Tris, 300 mM NaCl, 1mM DTT (dithiothréitol), 8M urea, pH 8) and lysed by ultrasonication. The supernatant containing the unfolded protein was applied to a HisTrap HP 5 ml affinity column (Cytiva, Freiburg im Breisgau, Germany). The His₆-tagged protein was eluted in 50 mM Tris, 300 mM NaCl, 1mM DTT, 8M urea, pH 8 with an imidazole gradient up to 500 mM. At this step, MAX67 was directly dialyzed against 25 mM Na Acetate, 2 mM DTT, pH 4.6 buffer in order to remove imidazole and urea, allowing the refolding of the protein. The His₆-tag was then cleaved off using the HRV 3C protease. For MAX60 and MAX47 refolding, the His-tagged proteins were dialyzed at 4°C in 0.18% ammonia solution, to avoid protein precipitation during the re-folding process at pH 4.6. The His₆ tag was then cleaved out directly at pH 8. Ammonia was removed by lyophilization and the lyophilized samples were dissolved into 25 mM Na Acetate, 2 mM DTT, pH 4.6 buffer. All samples were then concentrated using Amicon Ultra Centrifugal Filter Devices (MW cutoff 3,000 Da), (Merck Millipore, Burlington, USA) prior to size exclusion chromatography (SEC) using HiLoad 16/600 Superdex 75 pg column (Cytiva). Fractions containing proteins were pooled, concentrated to 0.5 mM and stored at -20 °C.

NMR spectroscopy.

Samples for NMR measurements (200 μ L) were prepared at about 0.5 mM protein concentration in 25 mM Sodium Acetate buffer (pH 4.6), and 5% of D₂O was added for the deuterium lock.

¹H, ¹⁵N double-resonance and ¹H, ¹⁵N, ¹³C triple-resonance NMR experiments were performed at 32°C on Bruker AVANCE III 700 MHz and 800 MHz spectrometers equipped with a cryogenic Z-gradient ¹H-¹³C-¹⁵N 5 mm probe head. Backbone and C β resonance assignments were made using HNCA, HNCACB, CBCA(CO)NH, HNCO and HN(CA)CO standard experiments (Sattler et al. 1999) performed on the uniformly ¹⁵N/¹³C labeled samples. Side chains and H α proton resonance assignments were obtained through 3D [¹H, ¹⁵N] NOESY-HSQC (mixing time 150 ms) and TOCSY-HSQC (isotropic mixing: 60 ms) experiments. Water suppression was achieved with the WATERGATE sequence (Piotto et al. 1992). ¹H chemical shifts were directly referenced to the methyl resonance of DSS (2,2-Dimethyl-2-silapentane-5-sulfonate, Sodium salt), while ¹³C and ¹⁵N chemical shifts were referenced indirectly to the absolute frequency ratios ¹⁵N/¹H = 0.101329118 and ¹³C/¹H = 0.251449530.

Extent of Assignments and data deposition.

The data sets allowed the assignment of 90.9%, 97.3% and 99.7% of the proton resonances, 95.5%, 98.8% and 98.3% of the nitrogen resonances (amide groups), and 94.0%, 98.1% and 99.4% of the carbon resonances (C α , C β and C γ) for MAX47, MAX60 and MAX67, respectively. The assignments are deposited in the BMRB under accession numbers 34731 (MAX47), 34730 (MAX60) and 34729 (MAX67). The good signal dispersion observed in the [¹H, ¹⁵N] HSQC for these three proteins (Fig.1) is consistent with well-folded 3D structures. Interestingly, we observed two cross-peaks for each residue in the C-terminal segment (E98-W106) of MAX60, with relative intensities of 0.45:0.55. Probably, the cis-trans isomerization of one or two of the proline residues that flank W106 in the C-terminus (P104-F105-W106-P107) induces two different orientations for the tryptophan aromatic side-chain, yielding two different chemical environments for the neighboring residues.

TALOS-N (Shen & Bax 2013) analysis suggests a high content in extended β -strands in the 3D structure of the three proteins, consistent with the secondary structure of the MAX-effectors (Fig.1). In addition, Φ/Ψ values determined for residues Y91-E102 in MAX60 indicate the presence of an α -helix in the C-terminal end of the protein. These conclusions are further supported by CSI 3.0 analysis (Hafsa et al. 2015). The consensus chemical shift index derived from ¹H α , ¹³C α , ¹³C β , ¹³C γ and ¹⁵N¹H chemical shifts also supports the presence of five β -strands in the 3D structure of the three proteins, compatible with the β -sandwich structure shared by MAX effectors. Also, CSI analysis supports the presence of an α -helix in the C-terminal end of MAX60 (See Supplementary Material, Fig.S1). At this step, we have no precise idea about the role of this C-terminal helical extension in the function of the effector, even if we suspect that it might confer some target specificity to MAX60 with regard to others MAX effectors. This assumption has to be further supported with NMR in-vitro interaction studies with potential effector targets, once the solution structure of this effector will be solved.

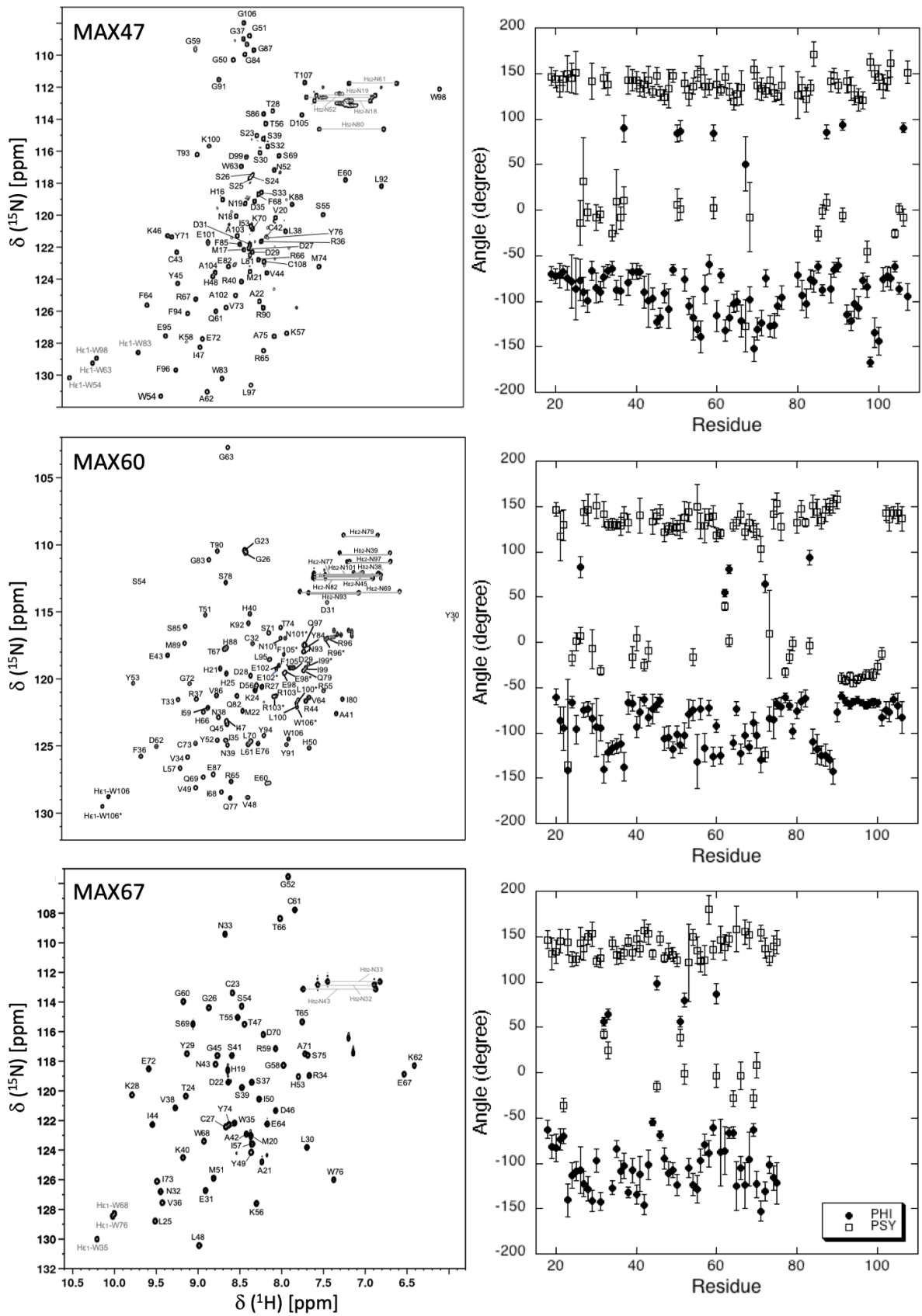


Figure 1: (Left) 2D ^1H - ^{15}N HSQC spectra of MAX47, MAX60 and MAX67 (from top to bottom, as indicated) recorded at 700 MHz on ^{15}N -uniformly labeled samples dissolved in 25 mM Sodium Acetate buffer pH 4.6 at 32°C. Cross peak assignments are indicated using the one-letter amino acid code and number. The sequence

numberings correspond to the full-length proteins, including the signal peptide. (Right) Corresponding plots of the Φ (bold circles) / Ψ (open squares) dihedral angle values obtained from TALOS-N (Shen & Bax 2013) analysis of the chemical-shifts measured for the three proteins.

Statements and declarations.

***Ethics approval and consent to participate:** Not applicable

***Consent for publication:** Not applicable

***Availability of data and material:** Assignments have been deposited to and are available from the BMRB data bank.

***Competing interests:** The authors declare no conflict of interest.

***Funding:** This project was funded by the ANR project MagMAX (ANR-18-CE20-0016-02) and supported by French Infrastructure for Integrated Structural Biology (FRISBI) grant No. ANR-10-INSB-05.

***Authors' contributions:** M.L., K.d.G., J.P., and M.R. sub-cloned, expressed and purified the three recombinant proteins.

M.L. recorded and analyzed the NMR spectra with P.B., C.R. and A.P. She also prepared the figure and contributed to the writing.

S.C. and P.G. realized the data mining on Magnaporthe genome and characterized the protein sequences.

T.K., A.P. and C.R. got the funding for this research work.

CR and PB wrote the manuscript.

All authors reviewed the manuscript.

References.

Araújo LGD, Prabhu AS, Freire ADB (2000) Development of blast resistant somaclones of the upland rice cultivar araguaia. *Pesq agropec bras* 35:357–367. <https://doi.org/10.1590/S0100-204X2000000200015>

Bentham AR, Petit-Houdenot Y, Win J, et al (2021) A single amino acid polymorphism in a conserved effector of the multihost blast fungus pathogen expands host-target binding spectrum. *PLoS Pathog* 17:e1009957. <https://doi.org/10.1371/journal.ppat.1009957>

Couch BC, Fudal I, Lebrun M-H, et al (2005) Origins of Host-Specific Populations of the Blast Pathogen *Magnaporthe oryzae* in Crop Domestication With Subsequent Expansion of Pandemic Clones on Rice and Weeds of Rice. *Genetics* 170:613–630. <https://doi.org/10.1534/genetics.105.041780>

de Guillen K, Ortiz-Vallejo D, Gracy J, et al (2015) Structure Analysis Uncovers a Highly Diverse but Structurally Conserved Effector Family in Phytopathogenic Fungi. *PLoS Pathog* 11:e1005228. <https://doi.org/10.1371/journal.ppat.1005228>

De la Concepcion JC, Franceschetti M, Maqbool A, et al (2018) Polymorphic residues in rice NLRs expand binding and response to effectors of the blast pathogen. *Nature Plants* 4:576–585. <https://doi.org/10.1038/s41477-018-0194-x>

De la Concepcion JC, Maidment JHR, Longya A, et al (2021) The allelic rice immune receptor Pikh confers extended resistance to strains of the blast fungus through a single polymorphism in the effector binding interface. *PLoS Pathog* 17:e1009368. <https://doi.org/10.1371/journal.ppat.1009368>

Dean R, Van Kan JAL, Pretorius ZA, et al (2012) The Top 10 fungal pathogens in molecular plant pathology: Top 10 fungal pathogens. *Molecular Plant Pathology* 13:414–430. <https://doi.org/10.1111/j.1364-3703.2011.00783.x>

Doehlemann G, Requena N, Schaefer P, et al (2014) Reprogramming of plant cells by filamentous plant-colonizing microbes. *New Phytol* 204:803–814. <https://doi.org/10.1111/nph.12938>

Eseola AB, Ryder LS, Osés-Ruiz M, et al (2021) Investigating the cell and developmental biology of plant infection by the rice blast fungus *Magnaporthe oryzae*. *Fungal Genetics and Biology* 154:103562. <https://doi.org/10.1016/j.fgb.2021.103562>

- Fernandez J, Orth K (2018) Rise of a Cereal Killer: The Biology of *Magnaporthe oryzae* Biotrophic Growth. *Trends in Microbiology* 26:582–597. <https://doi.org/10.1016/j.tim.2017.12.007>
- Giraldo MC, Dagdas YF, Gupta YK, et al (2013) Two distinct secretion systems facilitate tissue invasion by the rice blast fungus *Magnaporthe oryzae*. *Nat Commun* 4:1996. <https://doi.org/10.1038/ncomms2996>
- Hafsa NE, Arndt D, Wishart DS (2015). CSI 3.0: a web server for identifying secondary and super-secondary structure in proteins using NMR chemical shifts, *Nucleic Acids Research*, 43:W370-377. <https://doi.org/10.1093/nar/gkv494>
- Hogenhout SA, Van der Hoorn RAL, Terauchi R, Kamoun S (2009) Emerging Concepts in Effector Biology of Plant-Associated Organisms. *MPMI* 22:115–122. <https://doi.org/10.1094/MPMI-22-2-0115>
- Houterman PM, Cornelissen BJC, Rep M (2008a) Suppression of Plant Resistance Gene-Based Immunity by a Fungal Effector. *PLoS Pathog* 4:e1000061. <https://doi.org/10.1371/journal.ppat.1000061>
- Jones JDG, Dangl JL (2006) The plant immune system. *Nature* 444:323–329. <https://doi.org/10.1038/nature05286>
- Maidment JHR, Franceschetti M, Maqbool A, et al (2021) Multiple variants of the fungal effector AVR-Pik bind the HMA domain of the rice protein OshIPP19, providing a foundation to engineer plant defense. *Journal of Biological Chemistry* 296:100371. <https://doi.org/10.1016/j.jbc.2021.100371>
- Maqbool A, Saitoh H, Franceschetti M, et al (2015) Structural basis of pathogen recognition by an integrated HMA domain in a plant NLR immune receptor. *eLife* 4:e08709. <https://doi.org/10.7554/eLife.08709>
- Nyarko A, Singarapu KK, Figueroa M, et al (2014) Solution NMR Structures of *Pyrenophora tritici-repentis* ToxB and Its Inactive Homolog Reveal Potential Determinants of Toxin Activity. *Journal of Biological Chemistry* 289:25946–25956. <https://doi.org/10.1074/jbc.M114.569103>
- Ou SH (1980) Pathogen Variability and Host Resistance in Rice Blast Disease. *Annu Rev Phytopathol* 18:167–187. <https://doi.org/10.1146/annurev.py.18.090180.001123>
- Petre B, Kamoun S (2014) How Do Filamentous Pathogens Deliver Effector Proteins into Plant Cells? *PLoS Biol* 12:e1001801. <https://doi.org/10.1371/journal.pbio.1001801>
- Piotto M, Saudek V, Sklenar V (1992) Gradient-tailored excitation for single-quantum NMR spectroscopy of aqueous solutions. *J Biomol NMR* 1992, 2:661-665. <https://doi.org/10.1007/BF02192855>
- Ribot C, Césari S, Abidi I, et al (2013) The *Magnaporthe oryzae* effector AVR1-CO39 is translocated into rice cells independently of a fungal-derived machinery. *Plant J* 74:1–12. <https://doi.org/10.1111/tpj.12099>
- Sattler M, Schleucher J, Griesinger C (1999) Heteronuclear multidimensional NMR experiments for the structure determination of proteins in solution employing pulsed field gradients. *Prog Nucl Mag Reson Spectrosc* 34:93-158. [https://doi.org/10.1016/S0079-6565\(98\)00025-9](https://doi.org/10.1016/S0079-6565(98)00025-9)
- Shen Y, Bax A (2013) Protein backbone and sidechain torsion angles predicted from NMR chemical shifts using artificial neural networks. *J Biomol NMR* 56:227–241. <https://doi.org/10.1007/s10858-013-9741-y>
- Wang X, Jiang N, Liu J, et al (2014) The role of effectors and host immunity in plant–necrotrophic fungal interactions. *Virulence* 5:722–732. <https://doi.org/10.4161/viru.29798>
- Zhang X, He D, Zhao Y, et al (2018) A positive-charged patch and stabilized hydrophobic core are essential for avirulence function of AvrPib in the rice blast fungus. *Plant J* 96:133–146. <https://doi.org/10.1111/tpj.14023>
- Zhang Z-M, Zhang X, Zhou Z-R, et al (2013) Solution structure of the *Magnaporthe oryzae* avirulence protein AvrPiz-t. *J Biomol NMR* 55:219–223. <https://doi.org/10.1007/s10858-012-9695-5>
- Zhang Z-M, Zhang X, Zhou Z-R, et al (2013) Solution structure of the *Magnaporthe oryzae* avirulence protein AvrPiz-t. *J Biomol NMR* 55:219–223. <https://doi.org/10.1007/s10858-012-9695-5>

